

A Numerical Simulation of Self-Gravitating Fluid Equations: Verification of Jeans Instability

Lorenzo Maria Perrone¹

Department of Physics, Ecole Polytechnique Federale de Lausanne EPFL, Lausanne ^{a)}

In this report, we will propose a one dimensional higher-order numerical scheme that simulates the Euler's equations for an isothermal self-gravitating sphere of gas. Our aim is to find numerically the size of the sphere at which the system becomes unstable under the action of a small perturbation, leading to gravitational collapse. This problem of astrophysical relevance is solved analytically in the context of perturbation theory around the point of equilibrium and it is known as *Jeans Instability*. With Jean's approach, one can find the frequency of the exponentially growing solution but, through the perturbative method, this solution is physically meaningful only a short time after the initial t_0 . With our numerical approach, instead - and under the assumptions stated above - it is possible to simulate the entire evolution of the gas sphere. In particular, we will look for a validation of the model using the analytical results available.

I. INTRODUCTION: SELF-GRAVITATING EULER'S EQUATIONS

The dynamics of fluid systems can be described by the Euler's equations, which are a set of non-linear hyperbolic equations in the coordinates ρ, \mathbf{v}, p, E , i.e. density, velocity field, pressure and energy. The application of Euler's equation is vast in many fields of physics, including the study of astrophysical fluids, such as clouds of gas or galactic flows. Their most general formulation is the following:

$$\frac{\partial \rho}{\partial t} + \nabla \cdot (\rho \mathbf{v}) = 0 \quad (1)$$

$$\frac{\partial \rho \mathbf{v}}{\partial t} + \nabla \cdot (\mathbf{v} \mathbf{v}^T \rho) = -\nabla p + \mathbf{s} \quad (2)$$

$$\frac{\partial \epsilon}{\partial t} + \mathbf{v} \cdot \nabla \epsilon + \frac{p}{\rho} \nabla \cdot \mathbf{v} = 0 \quad (3)$$

$$p = p(\rho), \quad (4)$$

where Eq. (2) can also be rewritten in (perhaps) a more clear way as: $\partial_t(\rho v_i) + \partial_j(v_j v_i \rho) = -\partial_i p + s_i$. In Eq. (2), s represents any external source that acts on the system. Eq. (4), generally known as *polytropic* equation, is a necessary closure to the coupled system of equations and it is usually enforced through physical considerations on the specific system which is being studied. The above equations well-fit fluid dynamics in absence of gravity field, either external - as in the case, for instance, of waves in the ocean - or internal, coming from a self-gravitating system as in our case. To account for the gravitational potential, a modification of Eq. (2) is needed and a complete system of equations will then become:

$$\frac{\partial \rho}{\partial t} + \nabla \cdot (\rho \mathbf{v}) = 0 \quad (5)$$

$$\frac{\partial \rho \mathbf{v}}{\partial t} + \nabla \cdot (\mathbf{v} \mathbf{v}^T \rho) = -\nabla p - \rho \nabla \Phi \quad (6)$$

$$\frac{\partial \epsilon}{\partial t} + \mathbf{v} \cdot \nabla \epsilon + \frac{p}{\rho} \nabla \cdot \mathbf{v} = 0 \quad (7)$$

$$p = p(\rho) \quad (8)$$

$$\nabla^2 \Phi = 4\pi G \rho, \quad (9)$$

where the last equation is the Poisson equation that relates the laplacian of the gravitational potential Φ to the density ρ through the Newton's gravitational constant G .

A. Brief Derivation of Jean's Instability

Starting from the fluid, self-gravitating Euler's equation, we assume the system to be in a configuration of equilibrium which is time-independent and we introduce a small fluctuation proportional to the parameter $\epsilon \ll 1$. The quantities of interest will be rewritten as:

$$\rho(\mathbf{x}, t) = \rho_0(\mathbf{x}) + \epsilon \rho_1(\mathbf{x}, t)$$

$$p(\mathbf{x}, t) = p_0(\mathbf{x}) + \epsilon p_1(\mathbf{x}, t)$$

$$\Phi(\mathbf{x}, t) = \Phi_0(\mathbf{x}) + \epsilon \Phi_1(\mathbf{x}, t)$$

$$\mathbf{v}(\mathbf{x}, t) = \mathbf{v}_0(\mathbf{x}) + \epsilon \mathbf{v}_1(\mathbf{x}, t).$$

We now proceed to the linearization of Eq. (5- 9) at first order in the expansion parameter ϵ . We will assume that the initial velocity $\mathbf{v}_0 = 0$ and that the equilibrium density profile is constant: $\rho_0(\mathbf{x}) = \rho_0$. To simplify the treatment of the system of equations, we will make the additional assumption that $\Phi_0 = 0$: this latter hypothesis, though not so physical, goes under the name of *Jean's swindle*¹. An analogous derivation of the gravitational instability can be done without this latter assumption but, nevertheless, even this simplistic model

^{a)} Electronic mail: lorenzo.perrone@epfl.ch

provides valuable insight.

The linearized equations will then be:

$$\frac{\partial \rho_1}{\partial t} + \rho_0 \nabla \cdot \mathbf{v}_1 = 0 \quad (10)$$

$$\frac{\partial \mathbf{v}_1}{\partial t} = \frac{1}{\rho_0} c_s^2 \nabla \rho_1 - \nabla \Phi_1 \quad (11)$$

$$4\pi G \rho_1 = \nabla^2 \Phi_1 \quad (12)$$

where $p_1 = \left(\frac{dp}{d\rho}\right)_0 \rho_1 \equiv c_s^2 \rho_1$. If we now derive the continuity equation by t , take the gradient of the moment equation and substitute, we end up with a second-order in time and in space partial differential equation in ρ_1 alone that reads:

$$\frac{\partial^2 \rho_1}{\partial t^2} - c_s^2 \nabla^2 \rho_1 - 4\pi G \rho_0 \rho_1 = 0, \quad (13)$$

which of course has to be coupled with Poisson's equation. For these equations, we will seek a solution in Fourier's space by expanding the density perturbation as: $\rho_1(\mathbf{x}, t) = C e^{i\mathbf{k} \cdot \mathbf{x} - \omega t}$. By substituting in Eq. (13) we find for ω the following value:

$$\omega^2 = c_s^2 k^2 - 4\pi G \rho_0. \quad (14)$$

Clearly, if $\omega^2 < 0$, an unstable solution appears in the Fourier expansion as $\rho_1 \sim e^{+|\omega|t}$, which is related to the wavelength $\lambda_J^2 = \pi c_s^2 / G \rho_0$, that is called "Jean's length". This growing mode tells us that perturbations that act on a scale which is larger than the Jean's length will result in a collapse of the cloud of gas in which the outward pressure is not able to sustain the gravitational attraction anymore. This phenomenon is at the core of processes that have led to the formation of very hot and dense clouds that eventually became stars, and therefore it is of primary importance in astrophysical mechanisms. We would like to remark that the above results are only valid for *non-rotating* systems, while centrifugal forces would have to be taken into account for the rotating case.

B. Euler's Equations in the Simulation

In the following discussion we will make the following assumptions that will simplify greatly the equations to evolve. Firstly, we will make the hypothesis of an isotropic cloud of gas symmetric with respect to the origin of the reference system. We will therefore analyze only a *slice* of the cloud extending in one dimension in Cartesian coordinates, say x . This will make the differential operators in Eq. (5-9) much easier to treat. An alternative approach would be to use the isotropy assumption to go to radial coordinates, thus enforcing the symmetry between $x \leftrightarrow -x$ already

in the formulation of the equations. This option would halve the number of grid-points needed to achieve the same accuracy but would also require a less-immediate re-formulation of the conserved variables to take into account the additional terms coming from the differential operators in spherical coordinates. For additional comments, cf.⁵.

A second simplification is the assumption of isothermal gas, which follows from a specific choice of the polytropic. Indeed, in a general polytropic we have a dependence of p on ρ of the kind $p = \text{const} \rho^{(n+1)/n}$, where n is called *polytropic index*. The isothermal assumption corresponds to choosing $n \rightarrow \infty$ and therefore $p = c_s^2 \rho$, where now the constant of proportionality has been rewritten as c_s^2 , which is the speed of sound. With the above assumptions, the energy density ϵ decouples and the only variables that we are left with are ρ, v :

$$\rho_t + (\rho v)_x = 0 \quad (15)$$

$$(\rho v)_t + (\rho v^2 + c_s^2 \rho)_x = -\rho \Phi_x \quad (16)$$

$$\Phi_{xx} = 4\pi G \rho, \quad (17)$$

where we adopted the notation $\partial/\partial t \rightarrow (\cdot)_t$. As we can see, the gravitational potential is uniquely determined by the density profile of the gas and has no temporal evolution of its own. For this reason, as it is customary⁴ in simulations of self-gravitating fluid dynamics for "body forces", Φ_x will be treated as an external source that depends on the variables of the system (in this case, ρ). For future reference, we note that a set of partial differential equations in the form of $\mathbf{u}_t + \mathbf{f}(\mathbf{u})_x = \mathbf{S}$ - as in (15) - is said to be in conservation form.

II. THE NUMERICAL SCHEME

When performing a numerical simulation of solutions of PDEs, one should always be particularly careful about potential issues coming from the use of an inadequate scheme and that could lead to poor accuracy or even non-physical results. This is even more the case when physical systems are being studied as the conservation laws under scrutiny describe the evolution of quantities - such as the energy or the velocity - that are fundamental to understand the behaviour of a system and to describe the physical reality. In particular, the possibility in non-linear equations that discontinuous solutions can be produced even from smooth initial conditions is a major fact that should be taken into account when devising a numerical scheme, along with the necessity to be able to pick the physical solution (called *entropy solution*) whenever multiple ones are mathematically allowed.

To overcome this potentially critical issues, a number of schemes and approaches have been devised over the years. In this project, we will adopt a scheme based on

the finite volume method, which averages the initial conditions over a grid of cells and then evolves the averages. The cell averages are defined as follows:

$$\bar{\mathbf{u}}_j^n = \frac{1}{\Delta x} \int_{x_{j-1/2}}^{x_{j+1/2}} \mathbf{u}(x, t^n) dx, \quad (18)$$

where j indicates the position on the N -point grid $j = 0, 1, \dots, N-1$, and n is the discretized time-step. An analogous discretization is made for the source term. We will use an “update formula” for the solution vector \mathbf{u} as the following:

$$\frac{\partial \bar{\mathbf{u}}_i}{\partial t} = -\frac{1}{\Delta x} [\mathbf{F}_{i+1/2} - \mathbf{F}_{i-1/2}] + \bar{\mathbf{S}}_i,$$

where the function $\mathbf{F}(\mathbf{u}, \mathbf{v}) \equiv \frac{\mathbf{f}(\mathbf{u}) + \mathbf{f}(\mathbf{v})}{2} - \frac{\lambda}{2}(\mathbf{v} - \mathbf{u})$ is known as the *local* Lax-Friedrich numerical flux. The value $\lambda(\mathbf{u}, \mathbf{v})$ is the upper bound of the maximum eigenvalue of the flux-Jacobian $\nabla_{\mathbf{u}} \mathbf{f}$ at the interface between two neighbouring cells and, for our problem, is equal to $\lambda = c_S + |v|$. A main advantage of this approach is that it can be proved that the conservation of the physical quantities (such as mass, density, energy...) is encoded directly in the formulation of the method and guaranteed at a discrete level. The vector of the solutions $\mathbf{u}(x, t)$ is defined as:

$$\mathbf{u} = \begin{bmatrix} \rho \\ \rho v \end{bmatrix}, \quad (19)$$

while the (physical) flux is:

$$\mathbf{f}(\mathbf{u}) = \begin{bmatrix} \rho v \\ \rho v^2 + c_S^2 \rho \end{bmatrix}. \quad (20)$$

Second order accuracy in space is reached by using the *MUSCL* piece-wise linear reconstruction of the solution: at each time step and inside each cell j we seek a solution of the form $\mathbf{u}(x) = \bar{\mathbf{u}}_j + \frac{x - x_j}{\Delta x} \delta \mathbf{u}_j$, i.e. we reconstruct \mathbf{u} as a linear function with constant slope $\delta \mathbf{u}_j$. The slope cannot be chosen arbitrarily if we want a scheme which is total variation diminishing (TVD), that is a property in which we are rightly interested if we do not want the scheme to develop high frequency oscillations. We leave for **Appendix A** the discussion of what an appropriate choice for $\delta \mathbf{u}$ might be. Having reconstructed the piecewise linear solution, we will compute the Lax-Friedrich numerical flux in the update formula at the left and right interface of each cell using $\mathbf{u}_{j+1/2}^- = \bar{\mathbf{u}}_j + 0.5 * \delta \mathbf{u}_j$ and $\mathbf{u}_{j+1/2}^+ = \bar{\mathbf{u}}_{j+1} - 0.5 * \delta \mathbf{u}_{j+1}$, thus $\mathbf{F}_{j+1/2} = \mathbf{F}(\mathbf{u}_{j+1/2}^-, \mathbf{u}_{j+1/2}^+)$ and analogously for $\mathbf{F}_{j-1/2}$.

High order accuracy in time is reached by using a 3^{rd} -order Runge-Kutta *Strong Stability Preserving* (SSP)

scheme which is implemented as follows; for a general formulation of the problem $\mathbf{u}_t = \mathbf{L}(\mathbf{u}, t)$ we have:

$$\begin{aligned} \mathbf{u}^{(1)} &= \mathbf{u}^n + \Delta t \mathbf{L}(\mathbf{q}^n, t^n) \\ \mathbf{u}^{(2)} &= \frac{3}{4} \mathbf{u}^n + \frac{1}{4} \left(\mathbf{u}^{(1)} + \Delta t \mathbf{L}(\mathbf{q}^{(1)}, t^n + k) \right) \\ \mathbf{u}^{(3)} &= \frac{1}{3} \mathbf{u}^n + \frac{2}{3} \left(\mathbf{u}^{(2)} + \Delta t \mathbf{L}(\mathbf{q}^{(2)}, t^n + k/2) \right) \\ \mathbf{u}^{n+1} &= \mathbf{u}^{(3)} \end{aligned}$$

The SSP Runge-Kutta scheme guarantees that the TVD property of the linear MUSCL reconstruction is kept also at higher order in time, thus providing us with a time-marching apparatus suitable to our task. The integration of the $t = 0$ initial conditions can be performed according to many numerical schemes. Since we are interested in achieving second-order accuracy in space, it is enough to approximate the cell average with the mid-point rule or with the average of the solution at the left and right interfaces. Both the above methods are order $O(\Delta x)$ but, since we are linearly reconstructing the solution in the cell at each time step with the MUSCL scheme, the overall accuracy is not affected and the finite volume method will yield $O(\Delta x^2)$ accuracy.

The time step k is not uniform, but is chosen at each iteration by finding the fastest velocity of the modes over all the mesh, which is given by $\lambda_{max} = c_S + |v_{max}|$. In so doing, we set the CFL condition equal to $CFL = 0.5$ and $k = CFL \Delta x / \lambda_{max}$. In this way, we make sure that the velocity of the scheme is never lower than the velocity of the solution.

Finally, following², the derivative of the gravitational potential Φ has been discretely approximated by:

$$(\Phi_x)_j = 4\pi G \sum_{i=0}^j \rho_i \Delta x - 2\pi G \sum_{i=0}^{N-1} \rho_i \Delta x, \quad (21)$$

where the boundary condition $(\Phi_x)_{i=0} = -(\Phi_x)_{i=N-1}$ has been used³.

III. SET-UP OF THE SIMULATION AND RESULTS

We will perform our simulation in a closed box of size $L = 2$, with $x = 0$ corresponding to the left boundary and $x = 1$ being the centre of symmetry. To carry out the numerical evolution, *ghost cells* have been introduced to the left and to the right of our domain with reflecting boundary conditions, i.e. $\rho_{i=-1} = \rho_{i=0}$, $v_{i=-1} = -v_{i=0}$ and similarly for ρ_N, v_N . The initial profile for the density $\rho(x, 0) \equiv \rho_0(x)$ is chosen to be a combination of sigmoids, symmetric w.r.t. $x = 1$, such that we effectively model a uniform sphere with constant density at the centre of the box with steep but smooth transition

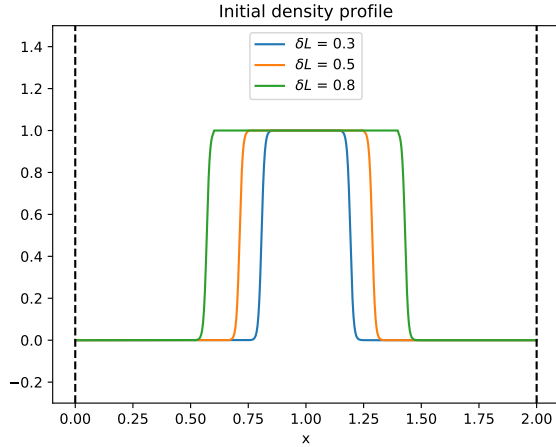


FIG. 1: Typical initial conditions for the density profile ρ_0 parametrized with $\delta L = 0.3, 0.5, 0.8$, which are coupled with zero initial velocity. The effective size of the gas sphere is very close to δL .

to the vacuum. This choice allows us to define easily a typical size of the system and a typical initial density that, for simplicity, has always been set to $\rho_T = 1$. An example of an initial condition for ρ_0 is in Fig. (1).

It seems evident that initial conditions of constant density profile cannot be equilibrium configurations of the self-gravitating Euler's equations. We expect, in fact, that soon after starting our simulation, the system will evolve reaching eventually some equilibrium and likely having small oscillations around it. It is also clear from the analytical derivation of Jean's instability that some simplifications (such as the Jean's swindle) are not represented in the numerical simulation. Furthermore, the assumption of small perturbation around equilibrium is not a easy to implement numerically. For these reasons, to validate our simulations, we will try to identify the initial size of the cloud with the scale of the perturbation and we will look for values of δL (typical size of the cloud) for which a collapse takes place. If these values of δL are comparable to the Jean's length within a reasonable range, we will say that the simulation has been successful. Finally, even if the cloud collapses, for evident reasons it will not be possible to simulate a *true* singularity at its core. We will discuss the implications of these caveats more in the next section.

For some initial conditions, the evolution of the cloud of gas can be really slow and it can take many iterations to converge to a new equilibria, which is the final snapshot we are interested in. To be sure to sample the right final density profiles, we will run long simulations (up to 10^5 iterations) during which we sample the maximum “height” of the density: if we see that at later times the sampled values are always in between

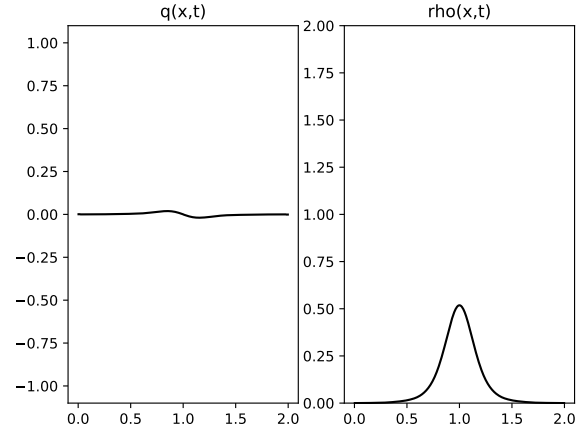


FIG. 2: Equilibrium solution for $\delta L = 0.1$ after 10^4 iterations. On the left panel the current (here called $q(x)$) is shown, while on the right panel we find the density profile. The current profile converges to zero if we increase the number of iterations.

two extrema, a maximum and a minimum, we can be rather certain that the true value of ρ_{max}^∞ is bounded by: $\rho_{max}^{t1} < \rho_{max}^\infty < \rho_{max}^{t2}$. Additionally, we can check the values of the velocity (we actually evolve the current ρv in the Euler's equations): when it settles close to zero we can be sure that the system has reached equilibrium (cf. Fig. (2)).

We choose units in which $G = 10$, and $c_S = 1$. For these values, Jean's length is $\lambda_J \sim 0.56$, if we consider an initial density of $\rho_0 = 1$.

In Fig. (3), we show the snapshots of the density profile for different choices of $\delta L = 0.3, 0.5, 0.8$ and after the 10^4 th iteration. As a first observation, it seems that the relation between ρ^∞ and δL is non-linear. We also show, in Fig. (4), the phenomenon of the small oscillations around the new equilibrium configuration after the cloud of gas has evolved for long enough.

To try to make a connection with the Jean's length, we will perform the following experiment: we will select a few values of δL between 0.1 and 1. For each of these values, we will run the simulation for $70e^4$ iterations, while sampling the maximum value of the density. We will then plot the sampled ρ^∞ against the effective size of the cloud (which, as we said, we “identify” with the scale of the perturbation). The result, in log-log scale, is in Fig. (5). We can observe immediately a power-law scaling with exponent ≈ 2 between ρ^∞ and δL , which is a hint of the non-linearity of our problem. More importantly, we see that for values of $\delta L \geq 0.3$, the cloud of gas tends to partially collapse in the core, reaching a new equilibrium state with $\rho_{max} > 1$. On the other hand, for

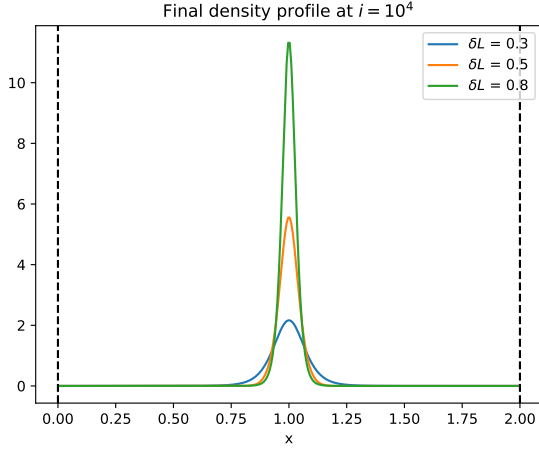


FIG. 3: Snapshots for the density profile ρ for $\delta L = 0.3, 0.5, 0.8$, and after 10000 iterations.

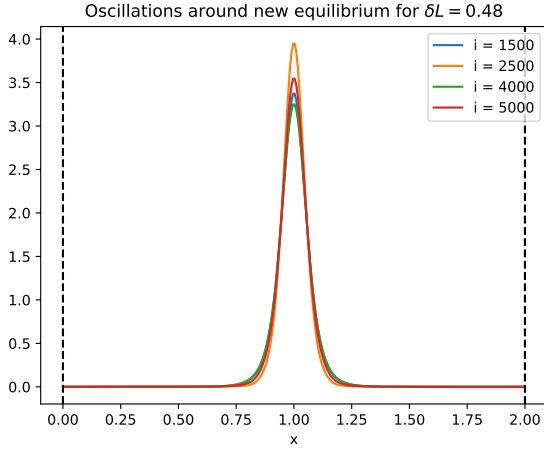


FIG. 4: Oscillations of the cloud density around a new equilibrium for $\delta L = 0.48$.

an initial extension of the cloud less than $\delta L = 0.3$, the cloud relaxes. Intuitively, we observe that we are finding a similar dynamics to the one described by Jeans: for a given initial density, the initial size of the system will determine if it will undergo collapse or small oscillations around a position of equilibrium. The fact that the dynamic of a medium (such as the gas) is not scale-invariant depends of course on the different functional dependence of the gravitational force and of the pressure on the size of the cloud, which is exactly the physical insight given by the Jean's instability.

IV. CONCLUSIONS

As we made it clear in the previous discussion, it is not possible to *exactly* retrieve Jean's results with a nu-

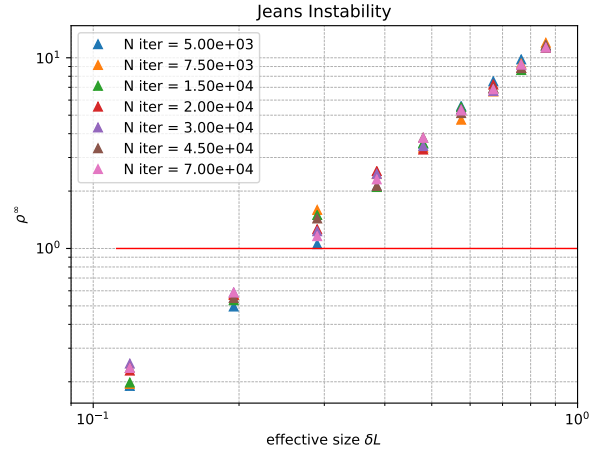


FIG. 5: Plot of the maximum height reached by clouds of gas with different initial extension. The red line represents the initial density ρ_0 which is the same for all the clouds.

merical simulation like the one set up in this report. The reasons are manifolds:

- the mathematical treatment of small oscillations in Fourier space is not analogous to the numerical simulation of Euler's equations. Moreover, the very idea of expanding around a configuration of equilibrium in Jean's treatment is not consistent with the assumptions of constant initial density and $\Phi_0 = 0$ (Jean's swindle). These are shortcomings of this simplified model which will affect the numerical results, but are accurate enough to describe the physical content;
- the Fourier expansion and the consequent instability which is found have a physical meaning only for a very short time after t_0 : no perturbation can grow exponentially for infinitely long times and, sooner or later, it saturates non-linearly. On the other hand, our simulation is carried on for longer times and, consequently, it is not straightforward to make connections with the theoretical description;
- we used the assumption that the sphere of gas is isothermal, i.e. $p \propto \rho$. This hypothesis simplifies our treatment but it not necessarily satisfied from a physical point of view as it would require that we can define a global temperature of the system. Moreover, we did not consider that *other* physical phenomena may take place during a sudden collapse of the core, such as radiative heating, fusion processes...

In the light of these considerations, we can claim that our model is sufficient to give insight on the dynamics behind the collapse (or not) of a cloud of gas but, given the many differences with Jean's treatment, it would not

be appropriate nor sensible to make comparisons with the analytical results. Nevertheless, the physical content of the two approaches is similar and the scales at which we observe (partial) collapse are comparable to the Jean's length. Additional bibliographic research on the simulation of Jean's instability via the self-gravitating Euler's equation has revealed that other fluid numerical approaches also lead to the same kind of conclusions.

V. STATEMENT OF THE AUTHOR

We hereby state that the work presented in this report is original and that all the bibliographic references consulted are properly listed. The content of this project has not been used for any courses other than the for the class of Computer Simulation of Physical Systems, with Prof. Pasquarello. The theory behind the numerical methods for conservation laws has been extensively treated in the course of Prof. Hestaven, while the theoretical derivation of Jean's instability has been carried out in the class of Prof. Kneib. The work in this report is to be considered a personal project that aims at using results and contents treated in multiple classes to study physical phenomena with a multi-disciplinary approach. The code is freely available on GitHub at the following address: <https://github.com/LorenzoLMP/Project-Jeans.git>.

Appendix A: Minmod

In this project, we apply the finite volume method in the space domain through the piecewise-linear reconstruction of the solution, i.e. we reconstruct \mathbf{u} as a linear function with constant slope $\delta\mathbf{u}_j$ inside each cell. Nevertheless, the slope cannot be chosen arbitrarily if we want a scheme which is total variation diminishing (TVD) and, therefore, we need a rule to help us pick the right slope inside each cell. The slope to use will depend on the left and right values at the interfaces: of the many possible choices available in literature, we will use the simple MIN-

MOD function. In the code, a MINMOD_GEN function has been implemented: it computes the slope in the following way:

$$\delta u_j = \quad (A1)$$

$$\text{minmod}(\Delta^-u_j, \Delta^+u_j) = \begin{cases} sg(\Delta^-u_j) \min(|\Delta^-u_j|, |\Delta^+u_j|) & \text{if } \Delta^-u_j * \Delta^+u_j > 0 \\ 0 & \text{otherwise} \end{cases} \quad (A2)$$

where $\Delta^-u_j = u_j - u_{j-1}$ and $\Delta^+u_j = u_{j+1} - u_j$. As we can see, if the difference at the interfaces have different sign on the left and right side (e.g., the cell in the middle has a cell averages which is lower than both its neighbouring cells), the slope will be put to zero. On the other hand, if the Δ s have same sign (the solution is either growing or decreases over all three cells) the slope is non zero: its sign will depend on the sign of the Δ^- , while its magnitude is chosen to be the minimum between the two deltas. By employing this slope limiter, we can find the appropriate forward and backward gradients such that no new minima or maxima is created, which would otherwise break the TVD property.

¹James Binney and Scott Tremaine. *Galactic Dynamics*. Princeton NJ Princeton University Press 1987 747 p, page 747, 1987.

²M. Colombeau. A consistent numerical scheme for self-gravitating fluid dynamics. *Numerical Methods for Partial Differential Equations*, 29(1):79–101, 2013.

³It is important to remark that, for the sake of numerical stability in very long runs, the vector of Φ_x is symmetrized with respect to the axis of symmetry $x = 1$ at each time step. In fact, it has been noticed that very small differences between the left and right vector potential eventually led the gas to migrate left or right.

⁴Eleuterio F. Toro. *Riemann Solvers and Numerical Methods for Fluid Dynamics*. 2009.

⁵Sheng Wang and Eric Johnsen. High-order schemes for cylindrical / spherical geometries with cylindrical / spherical symmetry. *AIAA Computational Fluid Dynamics Conference*, pages 1–10, 2013.